Structural Implication of Oxoammonium Cations for Reversible Organic One-electron Redox Reaction to Nitroxide Radicals

Yasunori Yonekuta, Kenichi Oyaizu, and Hiroyuki Nishide*
Department of Applied Chemistry, Waseda University, 3-4-1 Okubo, Shinjuku-ku, Tokyo 169-8555

(Received April 13, 2007; CL-070405; E-mail: nishide@waseda.jp)

Structures and electrochemical behaviors of nitroxide radicals reveal that their rapid and reversible redox reactions are based not only on their chemical stability but also on the increased sp^2 character of nitrogens which is intermediate between the purely sp^2 and sp^3 nitrogens in oxoammonium cations and amines, respectively.

Here, we report the first isolation and structure determination of oxoammonium cations, which provide insight into the nature of nitroxide radicals as the counterpart of the reversible $1e^-$ redox couple (Scheme 1).

Nitroxide radicals such as 2,2,6,6-tetramethylpiperidine-1-oxyl (TEMPO, **1**) have enjoyed widespread applications as spin-label and spin-trap agents for analytical purposes,[1] because of their stability under ambient conditions.[2] Studies on nitroxides have also been stimulated by their redox activities, which have spawned many metal-free redox catalysts for green technology,[3] organic magnetic materials based on spin alignment,[4] and electroactive materials for rechargeable energy-storage devices.[5] Recent trends involve the use of nitroxides as hole transport materials, which is believed to function by the nitroxide/oxoammonium couple.[6] Indeed, the reversible $1e^-$ oxidation of nitroxides in electrolyte solutions, with heterogeneous electron-transfer rate constants of more than 10^{-1} cm/s, has been established as a unique property of organic stable radicals,[7] although less attention has been paid to the property of oxoammonium cations.[8] We anticipated that how nitroxides experience changes in structure during the oxidation to the oxoammonium cation should unravel the origin of the rapid electron-transfer process. This paper reports our successful attempts to relate the energetic aspects of the redox reaction to the implications from the molecular structure, which was accessible by analysis of the crystal structures in both redox states.

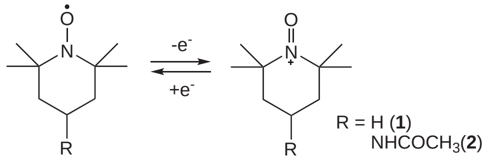

Scheme 1. Redox couples of nitroxide derivatives.

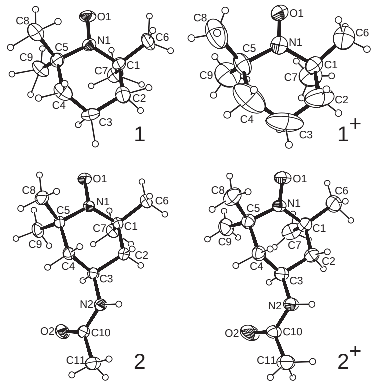

Figure 1. ORTEP drawings for the TEMPO derivatives (30% probability ellipsoids). Counter anions in $\mathbf{1}^+$ and $\mathbf{2}^+$ were omitted for clarity. Selected bond lengths (Å) and angles (deg). N1–O1: **1**, 1.284; $\mathbf{1}^+$, 1.184; **2**, 1.288; $\mathbf{2}^+$, 1.181. N1–C1: **1**, 1.472; $\mathbf{1}^+$, 1.527; **2**, 1.495; $\mathbf{2}^+$, 1.532. N1–C5: **1**, 1.501; $\mathbf{1}^+$, 1.532; **2**, 1.498; $\mathbf{2}^+$, 1.537. O1–N1–C1: **1**, 116.8; $\mathbf{1}^+$, 118.1; **2**, 115.9; $\mathbf{2}^+$, 118.5. O1–N1–C5: **1**, 114.9; $\mathbf{1}^+$, 117.5; **2**, 124.6; $\mathbf{2}^+$, 118.0. Deviation of N1 from O1–C1–C5 plane (Å): **1**, 0.1765; $\mathbf{1}^+$, 0.0073; **2**, 0.1641; $\mathbf{2}^+$, 0.0034.

Figure 1 shows the crystal structures of **1** and 4-acetamide-2,2,6,6-tetramethylpiperidine-1-oxyl (**2**), together with those of their oxidized products $[\mathbf{1}^+][BF_4]$ and $[\mathbf{2}^+][BF_4]$. The chemical oxidation of **1** and **2** was accomplished by aerobic oxidation in the presence of HBF_4 to give orange and bright yellow crystals, respectively. Single crystals were grown from CH_3CN solutions except **1**, for which sublimation was used as a method of crystallization. The atomic arrangement around the nitrogen atom revealed the electronic state of the N–O redox center. The N–O bond significantly shrank upon the oxidation by ca. 0.1 Å, as a result of an increased bond order in the oxoammonium cations compared with those of the radicals (N=O: 2-methyl-2-nitrosopropane, 1.199 Å).[9] Added support for this interpretation was provided by IR spectroscopy. The IR spectra of **1** and **2** exhibited intense peaks corresponding to the nitroxide radicals, with N–O stretching vibrations at 1465 and 1460 cm^{-1}, respectively. On the other hand, $[\mathbf{1}^+][BF_4]$ and $[\mathbf{2}^+][BF_4]$ showed corresponding peaks at 1626 and 1632 cm^{-1}, respectively. The shift was clearly indicative of the N–O double bond character in $[\mathbf{1}^+][BF_4]$ and $[\mathbf{2}^+][BF_4]$. Furthermore, the substantial absence of nitrogen displacement from C_2O (i.e., O1–C1–C5) plane in $[\mathbf{1}^+][BF_4]$ and $[\mathbf{2}^+][BF_4]$, which were only 0.0073 and 0.0034 Å, respectively, demonstrated the sp^2 character of their nitrogen atoms. These results, combined with the electrochemical data (vide infra), concluded that the oxoammonium cations were involved in the redox couple of **1** and **2** as shown in Scheme 1. Another curious feature of the oxoammonium cations is their high thermal stability. The decomposition of $[\mathbf{1}^+][BF_4]$ and $[\mathbf{2}^+][BF_4]$ was initiated at temperatures higher than 181 and 198 °C, respectively. The stability against thermolysis would promise their use as, e.g., redox catalysts and battery electrodes even at elevated temperatures when bound to polymer backbones.

The cyclic voltammograms of $[\mathbf{1}^+][BF_4]$ at various scan rates are shown in Figure 2a, which reveal a reversible wave at $(E_{pa} + E_{pc})/2 = 0.67$ V vs. Ag/AgCl with $\Delta E_p = E_{pa} - E_{pc} = 60$ mV at small scan rates that was close to the theoretical

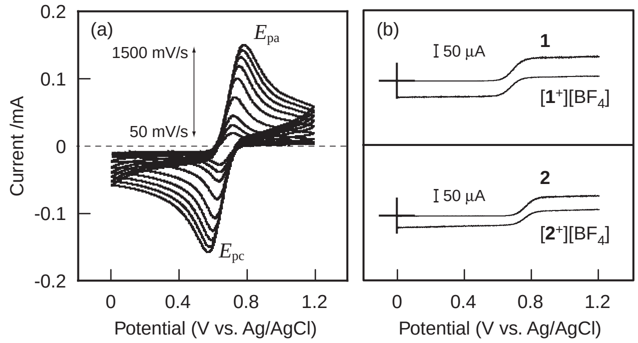

Figure 2. (a) Cyclic voltammograms of [**1**$^+$][BF$_4$] (1.0 mM) in CH_3CN containing 0.1 M TBABF$_4$. Scan rates were 25, 50, 100, 250, 500, 750, 1000, 1250, and 1500 mV/s. A platinum disc ($A = 0.1256\,\mathrm{cm}^2$) was used as the working electrode. The formal potential of the ferrocene/ferrocenium redox couple was 0.45 V vs. this reference electrode. (b) Current–potential curves for the TEMPO derivatives in Scheme 1 obtained with the same electrode rotated at 500 rpm. Scan rate = 20 mV/s.

value of 59 mV. The redox potential obtained from the solution prepared by dissolving **1** was identical to that obtained with the oxidized product. Similar trends were found for the **2**/[**2**$^+$][BF$_4$] couple at $(E_{pa} + E_{pc})/2 = 0.76$ V.

The heterogeneous electron-transfer rate constant (k_0) was estimated by the Nicholson method,[10] based on the increase in ΔE_p at very high scan rates (>1000 mV/s) with carefully compensated electrolyte resistance, which was accomplished by the combination of positive feedback circuitry and digital simulation methods. The standard rate constant for the **1**/**1**$^+$ couple was 8.4×10^{-1} cm/s from the data in Figure 2a, which provided support for the proposed large k_0 for **1** preliminarily obtained using solutions prepared by dissolving **1**.[11] The k_0 for the **2**/**2**$^+$ couple was similarly determined to be 7.8×10^{-1} cm/s. The rapid electron transfer with electrodes is indeed advantageous for use as redox catalysts and electroactive materials, which is expected for the TEMPO derivatives with various substituents.

Figure 2b shows the current–potential curves for solutions prepared by dissolving the TEMPO derivatives in Figure 1 recorded at a rotating disk electrode. The 1e$^-$ oxidation and reduction currents of the radical and the oxoammonium cation, respectively, appeared at the same half-wave potential for each redox couple. The Levich plots of limiting currents (i_L) vs. the square root of the electrode rotation rates (ω) were linear, as a result of the reversible character of the redox process at least at moderate rotation rates ($\omega < 2000$ rpm). Calculation of the diffusion coefficients (D) from the slope of the Levich plots ($i_L/\omega^{1/2}$) revealed that the charged species diffused more slowly (D: **1**$^+$, 2.6×10^{-5}; **2**$^+$, $2.2 \times 10^{-5}\,\mathrm{cm}^2$/s) than the pristine molecules (D: **1**, 3.4×10^{-5}; **2**$^+$, $2.6 \times 10^{-5}\,\mathrm{cm}^2$/s). The slight decrease in diffusion coefficients is ascribed to the increase in the solvation radii induced by the charging.

A question arises as to the origin of the rapid electron-transfer process of the TEMPO derivatives with electrodes. Organic molecules usually experience a large rearrangement of structural framework during the oxidation and reduction through the bond scission and formation that must overcome activation energies. Organic 1e$^-$ redox reactions found for, e.g., radicals stabilized by conjugated systems also suffer from resonance effects that contribute to slowing the electron transfer. On the other hand, the nitroxides are characterized by moderate delocalization of an unpaired electron over the N–O center. Consequently, the N–O bond is believed to have a partial π-bond character. Indeed, the nitrogen is slightly displaced from the C_2O plane by ca. 0.16 Å. The displacement is intermediate between the sp^3 amines (0.58 Å) and the oxoammonium cations, and is indicative of the partial sp^2 charatcter of the nitrogen in the nitroxides. A plausible account for the rapid redox reaction is given by the relatively small structural changes accompanied by the redox reaction, in addition to the stability of the radicals and the flexibility of the framework.

Another curious feature is the effect of the substituent at the 4-position of the nitroxide, which gives rise to a significant shift in the redox potential. The inductive effect of the acetamido substituent led to the positive shift in the potential by $\Delta E = 0.09$ V. The susceptibility to the substituent effect is the advantage of the organic molecules, in terms of matching the redox potentials for specific applications.

This work was partially supported by Grants-in-Aid for Scientific Research from NEXT, Japan. We thank Dr. M. Shiro for assistance in the crystallography of **1**.

References and Notes

1 a) P. J. Wright, A. M. English, *J. Am. Chem. Soc.* **2003**, *125*, 8655. b) P. P. Borbat, J. H. Davis, S. E. Butcher, J. H. Freed, *J. Am. Chem. Soc.* **2004**, *126*, 7746. c) K. Das, M. Pink, S. Rajca, A. Rajca, *J. Am. Chem. Soc.* **2006**, *128*, 5334.

2 A. R. Forrester, R. H. Thomson, *Nature* **1964**, *203*, 74.

3 a) M. F. Semmelhack, C. R. Schmid, D. A. Cortes, C. S. Chou, *J. Am. Chem. Soc.* **1984**, *106*, 3374. b) T. Osa, U. Akiba, I. Saegusa, J. M. Bobbitt, *Chem. Lett.* **1988**, 1423. c) F. Maccorquodale, J. A. Crayton, J. C. Walton, D. J. Worsfold, *Tetrahedron Lett.* **1990**, *31*, 771. d) A. Dijksman, A. Marino-gonzalez, A. M. i. Payeras, I. W. C. E. Arends, R. A. Sheldon, *J. Am. Chem. Soc.* **2001**, *123*, 6826. e) S. Tsujimoto, T. Iwahama, S. Sakaguchi, Y. Ishii, *Chem. Commun.* **2001**, 2352. f) Y. kashiwagi, T. Nishimura, J. Anzai, *Electrochim. Acta* **2002**, *47*, 1317.

4 a) E. Fukuzaki, H. Nishide, *J. Am. Chem. Soc.* **2006**, *128*, 996. b) T. Makarova, F. Palacio, *Carbon-Based Magnetism*, Amsterdam, Elsevier, **2006**. c) F. Iwahori, K. Kamibayashi, Y. Nishikawa, M. Yamashita, J. Abe, *Chem. Lett.* **2004**, *33*, 1460.

5 a) H. Nishide, S. Iwasa, Y.-J. Pu, T. Suga, K. Nakahara, M. Satoh, *Electrochim. Acta* **2004**, *50*, 827. b) T. Suga, H. Konishi, H. Nishide, *Chem. Commun.* **2007**, 1730. c) H. Nishide, T. Suga, *Electrochem. Soc. Interface* **2005**, *14*, 32. d) T. Suga, Y.-J. Pu, S. Kasatori, H. Nishide, *Macromolecules* **2007**, *40*, 3167.

6 T. Kurata, K. Koshika, F. Kato, J. Kido, H. Nishide, *Chem. Commun.* **2007**, doi:10.1039/b703790b.

7 a) E. Drockenmuller, J. M. Catala, *Macromolecules* **2002**, *35*, 2461. b) A. Israeli, M. Patt, M. Oron, A. Samuni, R. Kohen, S. Goldstein, *Free Radical Biol. Med.* **2005**, *38*, 317.

8 M. Schämann, H. J. Schäfer, *Electrochim. Acta* **2005**, *50*, 4956.

9 V. Pilepić, S. Uršić, *J. Mol. Struct.* **2001**, *538*, 41.

10 A. J. Bard, L. R. Faulkner, *Electrochemical Methods: Fundamentals and Applications*, 2nd ed., John Wiley & Sons, **2001**.

11 T. Suga, Y.-J. Pu, K. Oyaizu, H. Nishide, *Bull. Chem. Soc. Jpn.* **2004**, *77*, 2203.

12 Supporting information is available electronically on the CSJ-Journal Web site, http://www.csj.jp/journals/chem-lett.

Published on the web (Advance View) June 9, 2007; doi:10.1246/cl.2007.866